

Evaluating strategies to improve process efficiency of denitrification-based MICP

Pham, Vinh Phu; van Paassen, Leon A.; van der Star, Wouter R.L.; Heimovaara, Timo J.

DOI

[10.1061/\(ASCE\)GT.1943-5606.0001909](https://doi.org/10.1061/(ASCE)GT.1943-5606.0001909)

Publication date

2018

Document Version

Final published version

Published in

Journal of Geotechnical and Geoenvironmental Engineering

Citation (APA)

Pham, V. P., van Paassen, L. A., van der Star, W. R. L., & Heimovaara, T. J. (2018). Evaluating strategies to improve process efficiency of denitrification-based MICP. *Journal of Geotechnical and Geoenvironmental Engineering*, 144(8), Article 04018049. [https://doi.org/10.1061/\(ASCE\)GT.1943-5606.0001909](https://doi.org/10.1061/(ASCE)GT.1943-5606.0001909)

Important note

To cite this publication, please use the final published version (if applicable).
Please check the document version above.

Copyright

Other than for strictly personal use, it is not permitted to download, forward or distribute the text or part of it, without the consent of the author(s) and/or copyright holder(s), unless the work is under an open content license such as Creative Commons.

Takedown policy

Please contact us and provide details if you believe this document breaches copyrights.
We will remove access to the work immediately and investigate your claim.

Green Open Access added to TU Delft Institutional Repository

'You share, we take care!' – Taverne project

<https://www.openaccess.nl/en/you-share-we-take-care>

Otherwise as indicated in the copyright section: the publisher is the copyright holder of this work and the author uses the Dutch legislation to make this work public.

Evaluating Strategies to Improve Process Efficiency of Denitrification-Based MICP

Vinh Phu Pham, Ph.D.¹; Leon A. van Paassen, Ph.D., Aff.M.ASCE²;
Wouter R. L. van der Star, Ph.D.³; and Timo J. Heimovaara, Ph.D.⁴

Abstract: Microbially induced carbonate precipitation (MICP) through denitrification can potentially be applied as a bio-based ground improvement technique. Two strategies involving multiple batch treatments in a modified triaxial test setup were used to study the process efficiency. Both strategies aim to achieve 1 weight percentage (% by weight) of precipitated calcium carbonate (CaCO₃) and differ in number of flushes, hydraulic residence time, and substrate concentrations. In the experiment with few flushes and high substrate concentrations the microbial process was inhibited, only 0.28% by weight CaCO₃ was measured in the sand after 5 weeks of treatment. The regime with many flushes and low substrate concentrations stimulated microbial growth resulting in 0.65% by weight CaCO₃ within the same time period. Biomass growth and nitrogen gas production were stable throughout the experiment at low concentration, reducing the hydraulic conductivity of the sand, which eventually led to clogging. Precipitation rates up to 0.26% by weight/day CaCO₃ were observed. Applying a suitable substrate regime and residence time is important to limit inhibition and maintain the cell activity, allow for an efficient conversion, and generate a good precipitation rate. DOI: 10.1061/(ASCE)GT.1943-5606.0001909. © 2018 American Society of Civil Engineers.

Introduction

Microbially induced carbonate precipitation (MICP) is a potential method to improve soil characteristics and behavior for geotechnical and environmental applications. Various bacteria are able to induce carbonate precipitation by producing dissolved inorganic carbon (DIC) through their metabolism in an environment that has available nucleation sites, suitable pH, and sufficient supply of dissolved calcium. Dissimilatory nitrate reduction to dinitrogen gas, or denitrification, is one of these MICP processes, and has potential advantages of using waste streams for substrates, producing no by-products requiring removal, and making use of indigenous species of denitrifying bacteria (Van der Star et al. 2009). Denitrification consists of four sequential reduction steps from nitrate (NO₃⁻) to (di)nitrogen gas (N₂) through nitrite (NO₂⁻), nitric oxide (NO), nitrous oxide (N₂O): NO₃⁻ → NO₂⁻ → NO → N₂O → N₂, in which each step in the metabolic pathway is carried out by a different enzyme (van Spanning et al. 2007). Denitrifying bacteria generally have strategies to limit accumulation of the toxic intermediates (Ferguson 1994; Zumft 1997; van Spanning et al. 2007), so the measured concentrations of NO and N₂O are often far less than NO₂⁻ (Betlach and Tiedje 1981), making nitrite the only intermediate considered in studies in which denitrification is monitored.

One of the challenges of denitrification-based MICP is the low reaction rate compared with MICP through urea hydrolysis. MICP based on urea hydrolysis has been most widely studied and successfully demonstrated at large scale (DeJong et al. 2009; van Paassen et al. 2010b). It has shown to generate up to 6% by weight calcium carbonate within several treatment days (Whiffin et al. 2007; Burbank et al. 2011; Chu et al. 2012), whereas denitrification-based MICP needed several months up to a year to obtain an average 1–3% by weight (van Paassen et al. 2010a; O'Donnell 2016).

In wastewater treatment systems, nitrate with concentrations ranging from several millimoles per liter (Matějů et al. 1992) to more than 0.1 mol/L are treated, and nitrate removal rates of up to 31 mol/m³/day (Pinar et al. 1997) have been reported. If nitrate is assumed to be directly reduced to dinitrogen without accumulating the intermediates and all carbonate produced is used for CaCO₃, the precipitation rate can be calculated accordingly. The yield of DIC production over NO₃⁻ consumption (Y_{DIC}/Y_N) ranged from 1.25 to 1.45 (Pham et al. 2018). If calcium is in excess and all DIC is converted to CaCO₃, the amount of precipitated CaCO₃ per kilogram of soil with given dry density [ρ (kg/L)] and porosity (φ) is

$$w_{\text{CaCO}_3} = \frac{m_{\text{CaCO}_3}}{m_{\text{soil}}} = \frac{Y_{\text{DIC}} R_{\text{NO}_3^-} M_{\text{CaCO}_3}}{\frac{\rho_{\text{dry}}}{\varphi}} \quad (1)$$

where w_{CaCO_3} = weight fraction of CaCO₃ precipitated; $R_{\text{NO}_3^-}$ = NO₃⁻ consumption rate (mol/m³/day); and M_{CaCO_3} = 100 g/mol. Therefore, the nitrate removal rate of 31 mol/m³/day can theoretically result in a precipitation rate between 0.06 and 0.13% by weight/day depending on the reaction stoichiometry and the initial density and porosity of the sand. As several studies showed that 0.5 to 3% by weight of precipitated CaCO₃ can already help to increase the soil strength, especially at small strain (Montoya and DeJong 2015; Lin et al. 2016), denitrification-based MICP may have potential as ground improvement method or subsurface remediation (Martin et al. 2013) within a limited timeframe. The nitrogen gas, which is considered a side-product of denitrification-based MICP,

¹Researcher, Dept. of Geoscience and Engineering, Delft Univ. of Technology, Delft 2628 CN, Netherlands; Lecturer, Division of Geotechnology, Thuylou Univ., 175 Tay Son, Dong Da, 10000, Hanoi, Vietnam (corresponding author). ORCID: <https://orcid.org/0000-0002-4633-4490>. Email: vinhppham_p2v@outlook.com

²Associate Professor, School of Sustainable Engineering and the Built Environment, Arizona State Univ., Tempe, AZ 85281.

³Researcher, Subsurface and Groundwater Systems, Deltares, Utrecht 3584 BK, Netherlands.

⁴Professor, Dept. of Geoscience and Engineering, Delft Univ. of Technology, Delft 2628 CN, Netherlands.

Note. This manuscript was submitted on April 19, 2017; approved on January 22, 2018; published online on May 30, 2018. Discussion period open until October 30, 2018; separate discussions must be submitted for individual papers. This paper is part of the *Journal of Geotechnical and Geoenvironmental Engineering*, © ASCE, ISSN 1090-0241.

has an effect on the distribution and transport of the soluble substrates, and consequently limits the available substrates for denitrification and carbonate precipitation. In contrast, the induced gas phase may be a target on itself, considering that it decreases water saturation, which can help to enhance the soil resistance to dynamic loading and, for example, mitigate liquefaction (Rebata-Landa and Santamarina 2011; He et al. 2013; He and Chu 2014). Because of the low solubility of nitrogen gas, only very small amounts of gas need to be produced to improve the resistance to cyclic loading. The method can be considered as a two-stage process for liquefaction mitigation and has given promising results (Kavazanjian et al. 2015). According to this concept, first the induced gas dampens pore pressures and secondly the calcium carbonate minerals provide more durable strengthening.

The treatment protocol for denitrification-based MICP needs to consider several variables, among which are substrate concentrations and flushing frequency. Applying high substrate concentrations has the advantage that less frequent substrate supplies are required to reach the target amount of desired product. Nevertheless, for denitrification-based MICP, high substrate concentration may result in temporary or permanent nitrite accumulation, which leads to inhibition of further denitrification (Almeida et al. 1995; Glass and Silverstein 1998; Dhamole et al. 2007). In this study, the effect of the regime with which substrate is supplied on the efficiency of denitrification-based MICP is evaluated experimentally in sand columns under confined pressure conditions using a modified triaxial test setup. Two treatment protocols are evaluated, which both aimed to produce 1% by weight calcium carbonate in approximately 1 month: (1) using a low number of three flushes with relatively high substrate concentrations (50 mmol/L calcium nitrate—60 mmol/L calcium acetate) and a long hydraulic residence time of 10–12 days; and (2) using a high number of 15 flushes with low substrate concentration (10 mmol/L calcium nitrate—12 mmol/L calcium acetate) and a short hydraulic residence time of 2–3 days. The efficiency of the treatment is evaluated based on reaction rates, amount of precipitated CaCO_3 , the conversion of substrates, effect on the sand permeability, and drained response under monotonic loading.

Materials and Methods

Bacteria Cultivation

This study used denitrifying microorganisms that were enriched from a sample of the top soil from the Botanic garden of Delft University of Technology. They were enriched through six sequential liquid batch transfers using calcium salts of nitrate and acetate [30 mmol/L $\text{Ca}(\text{C}_2\text{H}_3\text{O}_2)_2$ to 25 mmol/L $\text{Ca}(\text{NO}_3)_2$], following the procedure presented by Pham et al. (2018). In the sixth batch, it took approximately 3 weeks for the nitrate to be completely consumed and for the newly accumulated nitrite to be depleted. After that, the suspension containing microorganisms was transferred to a new bottle by decantation, leaving out any visible crystals attached to the glass. To increase the reactivity of the inoculum, the bacteria were separated from the liquid by centrifugation. From the bottle, the liquid was evenly divided into 100-mL test tubes: a total of 4 tubes and centrifuged at 300 g (LKB 2610 Midispin centrifuge at 2,000 rpm) for 1.5 h. After centrifugation the supernatant was removed and the pellet containing microorganisms was collected by rinsing the test tubes with 5 mL of demi water. These cells were further incubated three more times in 30 mmol/L $\text{Ca}(\text{C}_2\text{H}_3\text{O}_2)_2$ to 25 mmol/L $\text{Ca}(\text{NO}_3)_2$ solution using the same procedure. At the last incubation, after 1.5 h centrifugation, the supernatant remained

turbid, indicating that there was still a significant number of suspended cells in the liquid in addition to the isolated biomass pellet in the bottom of the tubes. This supernatant was brought into new test tubes and centrifuged again for a total of 3 h until the liquid became clear and all cells were at the bottom. The remaining pellets after centrifuging were resuspended in a solution of 9 g/L NaCl, which was the stock inoculum for all of the following experiments. As a reference for the triaxial tests, a liquid batch experiment was performed using 15 mL stock inoculum in 380 mL of a suspension containing 26 mmol/L $\text{Ca}(\text{NO}_3)_2$ to 36 mmol/L $\text{Ca}(\text{C}_2\text{H}_3\text{O}_2)_2$. The same inoculum concentration (40 mL/L) was used for the incubations inside the triaxial test.

Sand Types

Baskarp sand (Sibelco, Antwerp, Belgium) was used in the experiments. Table 1 presents the properties of the batch that was used.

Substrate Concentrations, Number of Flushes, and Hydraulic Residence Time

Substrate solutions were prepared using demineralized water. The experiments used two regimes of substrate concentrations, in which the proportions of the two main substrates were kept equal but their concentrations varied:

- A high concentration regime using substrate concentrations of 50 mmol/L calcium nitrate [$\text{Ca}(\text{NO}_3)_2$] and 60 mmol/L calcium acetate [$\text{Ca}(\text{C}_2\text{H}_3\text{O}_2)_2$]; and
- A low concentration regime using substrate concentrations of 10 mmol/L calcium nitrate [$\text{Ca}(\text{NO}_3)_2$] and 12 mmol/L calcium acetate [$\text{Ca}(\text{C}_2\text{H}_3\text{O}_2)_2$].

Next to the main components, the solutions contained the following nutrients: 0.003 mmol/L $(\text{NH}_4)_2\text{SO}_4$, 0.0024 mmol/L MgSO_4 , 0.006 mmol/L KH_2PO_4 , 0.014 mmol/L K_2HPO_4 , and 1 mL/L trace element solution SL12B (Overmann et al. 1992) to avoid nutrient limitation during bacterial growth. The amount of substrate required to obtain 1% by weight of calcium carbonate in the sand samples can be calculated with an estimate of sample size, density and porosity, and assuming the denitrification and precipitation reactions were complete following the stoichiometry of maximum growth according to Pham et al. (2018). Accordingly, the high concentration regime required three flushes of substrate solution to reach the target amount of calcium carbonate, and the low concentration regime required 15 flushes.

The residence time, which is the duration between two flushes supplying fresh substrates, was determined based on conversion rates observed in earlier experiments (Pham et al. 2018). They are 10 days and 2–3 days for the high and low concentration regimes, respectively. To take into account a possible lag phase of bacterial growth to allow the population to adapt to the change of the substrate concentrations and the environment (from liquid

Table 1. Baskarp soil properties

Property	Value
10% pass particle size	0.083
d_{10} (mm)	
50% pass particle size	0.138
d_{50} (mm)	
Coefficient of uniformity, C_u	1.6
Coefficient of curvature, C_c	1.05
Void ratio	
e_{\max}	0.89
e_{\min}	0.55

to porous media), the first residence time was extended by 6 and 3 days for the high and low concentration regimes, respectively.

Equipment

A triaxial setup as shown in Fig. 1 was used for the experiments, which is similar to the one described in the ISO/TS 17892-9:2004 standard (CEN 2004). An additional third controller was connected to the inlet at the bottom of the sample and was placed at 1.5 m above the back pressure controller. Both the back pressure and inlet controllers were partly filled with liquid and the head space of both controllers was connected to the main pressure control, which allowed flushing the sand column from bottom to top at a defined back pressure under a constant head difference of 1.5 m (15 kPa above the pressure in the system). The back and inlet pressure controllers were put on balances to monitor change in the water mass while controlling pressure. In this way, the flow rate could be determined during flushing, to determine the hydraulic conductivity similar to a constant head test.

Experimental Procedure

The experiments were carried out according to the following procedure:

Sample Preparation

Sand columns were prepared using a split mold with the rubber membrane mounted inside (inner diameter = 65 mm and height = 130 mm). A 250-mL suspension was prepared containing the substrates together with 40 mL/L inoculum with the suspended bacteria. The suspension and the sand were poured into the mold in turns so that the sand level was always below the liquid level to avoid air entrapment. When the mold was nearly full, small amounts of liquid and sand were added until they filled up slightly above the top of the mold. The top part of the mold was slightly tamped to densify the excess sand and then the top surface was flattened to close the sample with a porous stone and the top cap. The resulting dry density of the samples was $1.48 \pm 0.01 \text{ g/cm}^3$, the porosity was 0.44 ± 0.003 , and the pore volume of the sample was approximately 0.2 L.

Saturation and Consolidation

The outer cell of the triaxial setup was installed and filled with water. The sample was pressurized to 200 kPa cell pressure

[100 kPa pore pressure using the procedure described in ISO/TS 17892-9:2004]. Then the back valve was opened for consolidation. Demineralized, de-aired water was used in the back pressure controller.

Reaction Phase

During the reaction phase, the back valve was opened to collect any expelled fluid in the back pressure controller. The amount of water expelled from the sample to the controller was continuously registered using a balance. The volume of expelled liquid during the reaction phase is assumed to be equal to the volume of gas formed inside the sample. Subsequently, the change in saturation was calculated assuming the porosity remained constant throughout the test and the sample was initially fully saturated with water.

Flushing

At the end of a reaction phase, the inlet controller was connected to the bottom line of the sample. This controller contained the new substrate solution, so when the inlet and back valves were opened, the sand column was flushed with fresh substrate from bottom to top with a 1.5-m water head gradient across the sample. In the experiment under the low concentration regime, the sample clogged during the 10th flush, which was removed by temporarily increasing the hydraulic gradient across the sample to 2.5 m by lowering the back pressure. Residual liquid in the sample was flushed to the back pressure controller and replaced by the fresh substrate solution. When the pore volume of the sample was completely replaced by the fresh solution, the inlet controller was disconnected by closing the inlet valve and the sample was left standing for the new reaction phase. The difference volume between injected and expelled liquid volumes was used to calculate the change in saturation. The pore pressure coefficient (or B-factor), which is the ratio of the change in pore pressure over the change in cell pressure and which is related to the degree of water saturation of the sample (Skempton 1954), was determined before and after flushing. The mass changes in the controllers measured by the balances were used to interpret the inflow and outflow rates. The inflow rate at the start and end of a flushing phase was used to determine the hydraulic conductivity at the constant hydraulic head.

The electrical conductivity (EC) of the effluent was monitored as an indicator for substrate conversion. During flushing, samples of the outflow were taken at regular time intervals for manual determination of EC and ion concentration. When taking the samples, the inlet and back valves were closed to temporarily stop flushing, the sampling valve was opened to let the first 1-mL liquid run through and collect the next 3 ml for sampling. Next, the sampling valve was closed, and the other two valves were reopened to continue flushing. Flushing continued until the EC of the outflow reached the value of the fresh substrate solution. The EC was measured using a SK10B electrode (Consort, Turnhout, Belgium) and recorded using a C3010 data logger (Consort). Nitrate, nitrite, and calcium concentrations were determined using a spectrophotometer (Lasa 100, Hach Lange, Loveland, Colorado) with standard test kits LCK339, LCK341 and LCK327, respectively. Acetate was determined using organic acid test kit LCK365, considering it was the only soluble source of organic carbon present in the samples.

To reach 1% by weight precipitated CaCO_3 in the sand, three times the substrate supply was required for the high concentration. The first supply was together with the inoculum when preparing the sample in the mold. From the second supply onward, fresh substrate was flushed through the sample. After flushing two times with fresh substrates, it was flushed the last time with de-aired demineralized water. The same approach was applied for the low concentration regime, except that the pore volume was flushed 14 times and then rinsed with de-aired demineralized water.

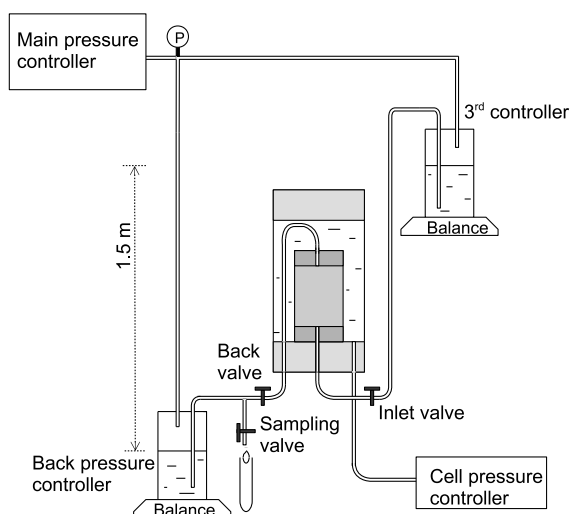


Fig. 1. Modified triaxial test setup used in the experiments.

Shearing

After rinsing the columns as described previously, the samples were sheared in compression under a constant confining pressure and drained conditions at a loading speed of 0.5 mm/min.

Posttreatment Analysis

After shearing, the sample was removed from the setup and cut into six slices, which were dried overnight at 105°C. After drying, the dried sand lumps were collected for further analysis using an environmental scanning electron microscope (ESEM, Philips ESEM XL30, Philips Electron Optics, Eindhoven, Netherlands). The CaCO_3 content was measured using a larger but similar setup to that of Whiffin et al. (2007). From each slice, approximately 100 g of the dried sample was placed in a closed bottle, to which 60 mL of a 100-g/kg hydrogen chloride (HCl) solution was added, allowing the CaCO_3 to dissolve. The produced CO_2 was collected

into an inverted 250-mL graduated cylinder placed in a water bath. When the reaction of CaCO_3 and HCl was finished, the cylinder height was adjusted to bring the gas pressure inside the cylinder back to ambient condition. The difference in gas volume inside the cylinder before and after the experiment corresponds to the volume of the produced CO_2 , V_{CO_2} (mL). The setup was calibrated using known amounts of CaCO_3 .

Results

Substrate Consumption of the Stock Inoculum in Liquid Batch

Using a stock inoculum concentration of 40 mL/L in a suspension containing 26 mmol/L $\text{Ca}(\text{NO}_3)_2$ to 36 mmol/L $\text{Ca}(\text{C}_2\text{H}_3\text{O}_2)_2$, it took 7 days for all nitrate to be consumed (Fig. 2). The NO_2^- concentration was below the detection level of 0.016 mmol/L throughout this period. After all of the NO_3^- was consumed, the residual acetate and calcium levels were approximately 40% of the initial values. A consumption of 42 mmol/L of acetate required 52 mmol/L nitrate consumption; consequently, the ratio between consumed acetate over nitrate was 0.8, similar to the ratio observed by Pham et al. (2018). The substrate consumption rate was 7.5 mmol/L/day for nitrate and 6.0 mmol/L/day for acetate.

Water Saturation Changes and Hydraulic Conductivity Reduction in the Triaxial Tests

Gas production in the setup resulted in a reduction of water saturation up to 75–80% of the pore volume in both the regimes for each reaction phase (Fig. 3). During the flushing with fresh substrate, it was not possible to remove all gas from pore space; the remaining gas phase stayed in the range of 10–15% after flushing (water saturation ranged from 85–90%). The unsaturated

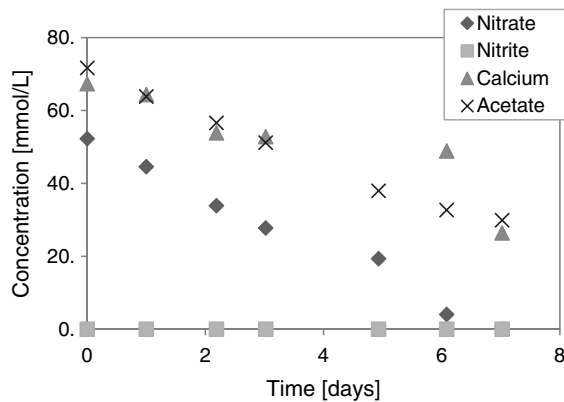


Fig. 2. Substrate concentrations during the incubation of the stock inoculum.

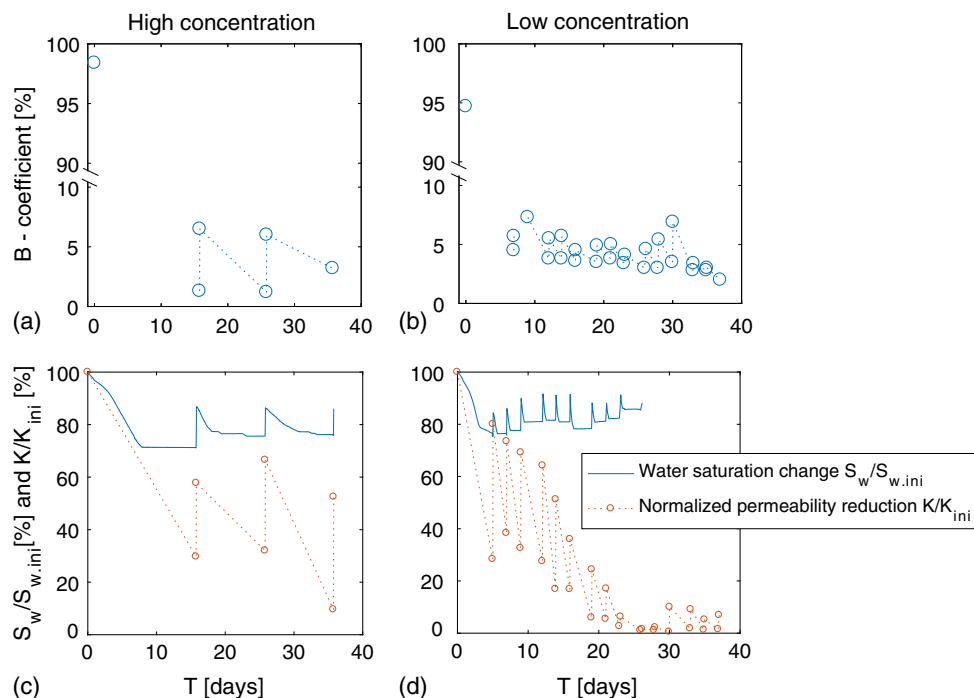


Fig. 3. B-coefficient variation of the samples at the end of each treatments in the (a) high concentration regime; and (b) low concentration regime; changes of water saturation during the treatment periods and the permeability at the end of each treatments in the (c) high concentration regime; and (d) low concentration regime.

condition was also reflected in the B-factor, which was below 10% throughout the experiments.

Gas production and the stability of the produced gas phase in the pore space had a significant effect on the hydraulic conductivity of the sand. However, a difference was observed between the two regimes. In the high concentration regime, gas production during the first period resulted in a reduction of more than two-thirds of hydraulic conductivity, half of which was regained after flushing; similar results were found for the subsequent flushes. In the low concentration regime, hydraulic conductivity was also partly regained after each flush, but subsequent treatments gradually led to clogging. At the 10th flush, the hydraulic conductivity had reduced by a factor of 200 compared with the initial conductivity. The resulting increase in water head from 1.5 to 2.5 m in the 11th and 13th (and the last flush to rinse the liquid through the sample) interrupted the flow to the back pressure controller. Therefore, monitoring the water balance was stopped after the 11th flush and the water saturation was not calculated any further (expelled liquid during the resident periods were still continuously monitored). The final value of the hydraulic conductivity of the treated sand in this regime was 5.8 cm/day, which was 15 times lower than the initial value.

Flow Rates during Flushing

Flow rates during flushing for the high and low concentration regimes are presented in Figs. 4 and 5, respectively.

All profiles show that the inflow started slowly, and outflow did not appear at the beginning of most of the flushes, but only occurred several seconds to minutes after the start of the flush. After this lag phase, the outflow rates increased to a level comparable with the inflow. During this period, treatments with the low concentration regime resulted in steady flows, whereas the flow rate in the treatments with the high concentration regime appeared to be irregular. The lag phase and irregular patterns in the observed flow rate for the high concentration regime may be due to relatively large trapped air pockets, which are gradually but irregularly flushed out. van Paassen et al. (2010a) observed similar irregular flow rates. Finally, for the high concentration regime, the final flow rate did not appear to be significantly affected, whereas for the low concentration regime the maximum flow rate during flushing gradually decreased, resulting in a decrease in hydraulic conductivity (Fig. 3).

Substrate Consumption and Production in the Sand Columns throughout the Treatments

There was a clear difference in the substrate consumption efficiency between the two regimes, as presented in Fig. 6.

In the high concentration regime, all acetate and most of the nitrate was consumed with small amounts of nitrite (<2 mmol/L) remaining in the first reaction phase, but in the subsequent reaction phases the conversion was much less efficient, resulting in significant amounts of residual solute substances in the setup and in the expelled liquid. During the second flush, almost 70% of the nitrate was consumed, but about half of that was not fully converted to dinitrogen gas and remained in the liquid as nitrite. The conversion in the third phase showed an even lower conversion, as only about 40% of the nitrate was consumed and the major part remained as nitrite in solution. Still, approximately 35% of the initial nitrate concentration in the second reaction phase and 20% in the third phase was not present as nitrate or nitrite in the effluent. It was assumed to be further reduced and converted to nitrogen gas, which corresponds to the observed expelled liquid and resulting reduction in the degree of saturation, as presented in Fig. 3. The low conversion efficiency was visible not only through substrate conversion, but also in the ratio of consumed acetate over nitrate (A/N), which decreased from the range that favors growth to the range where maintenance is dominant over growth (0.5 ± 0.05). At the end of the experiment, the average consumed acetate was about 15%, and the consumed nitrate NO_3^- was about 40% of the injected concentrations; however, a large fraction of it remained as the nitrite (about 50% and above). In case nitrite is remaining, the consumption ratio of acetate over total nitrate and nitrite, A/N^* , is used to evaluate the actual ratio between the carbon and nitrogen sources. For the second and third flush, correcting for the remaining nitrite results in the A/N^* of 0.9 and 1.1, respectively, compared with the A/N of 0.5.

The substrate consumption efficiency in the low concentration regime was retained throughout the experiment. With the initial supplied concentration of 20 mmol/L (5 mmol of nitrate in 250 mL pore volume), the remaining nitrate levels after 2 days were insignificant, and there was no detectable nitrite accumulation. The acetate to nitrate ratio (A/N) shifted slightly from 0.8:0.9 to 1.1:1.3 and was not different from the A/N^* , approaching a ratio that corresponds to the theoretical stoichiometry of maximum growth.

Using the measured substrate consumption ratios and amounts of left-over nitrite, the corresponding stoichiometry of the denitrification reaction can be calculated using the thermodynamic approach described by Heijnen and Kleerebezem (2010), assuming that nitrite is the only accumulating intermediate. Assuming the expelled volume of liquid during the reaction phase is equal to the volume of produced nitrogen gas, the conversion rate can be calculated from the flow rate at which the liquid is expelled during the reaction phase using the ideal gas law. Accordingly, deriving the stoichiometric coefficients from the observed substrate consumption ratio, the nitrate consumption and total DIC production

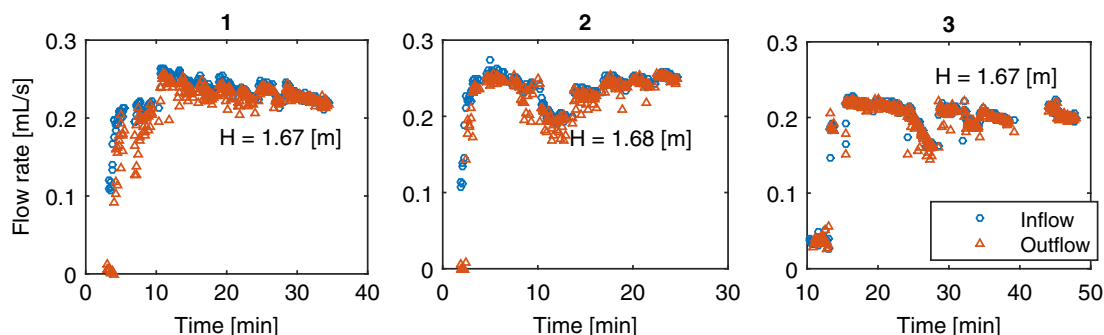


Fig. 4. Flow rates during flushing after each treatment in the high concentration regime.

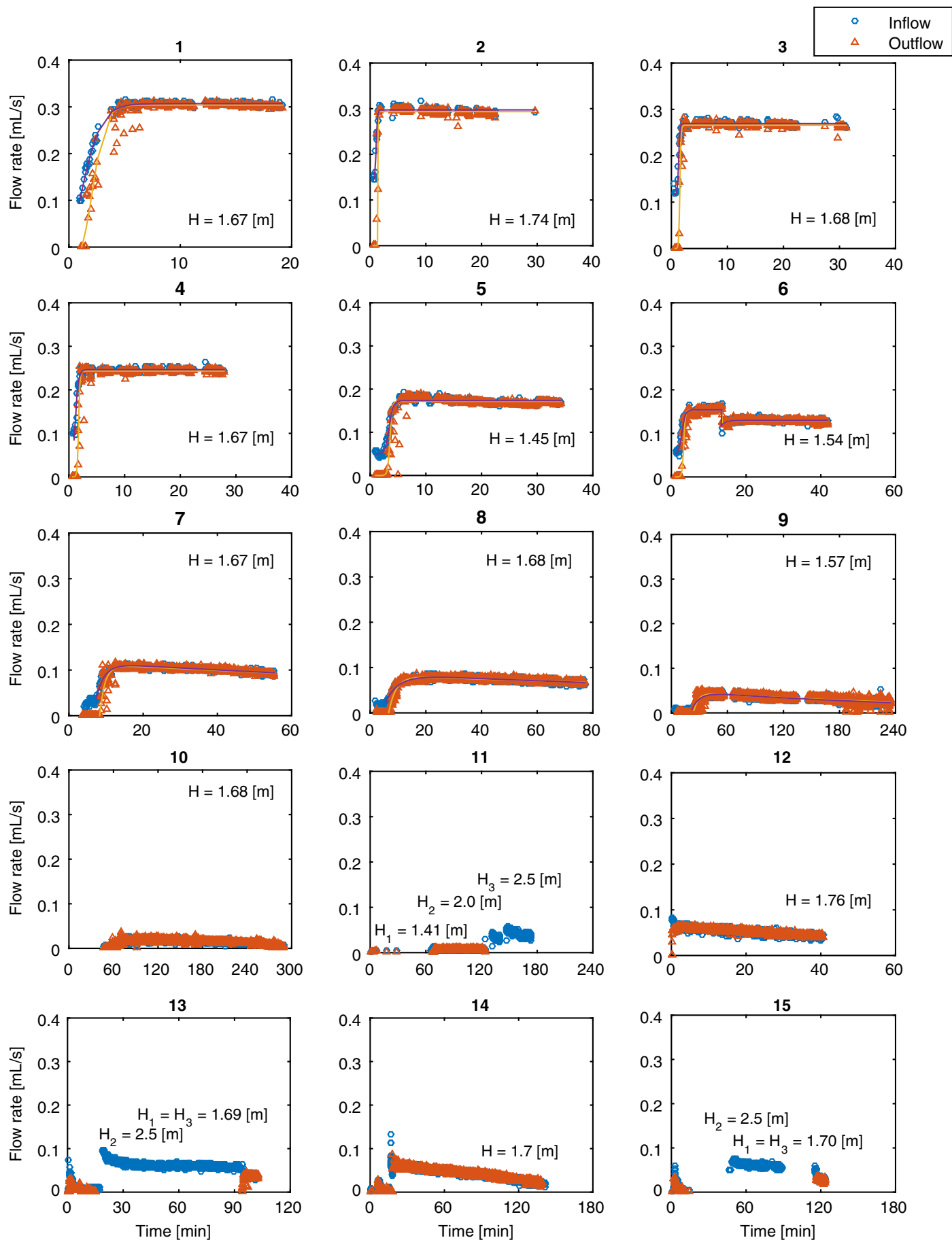


Fig. 5. Flow rates after each treatment in the low concentration regime.

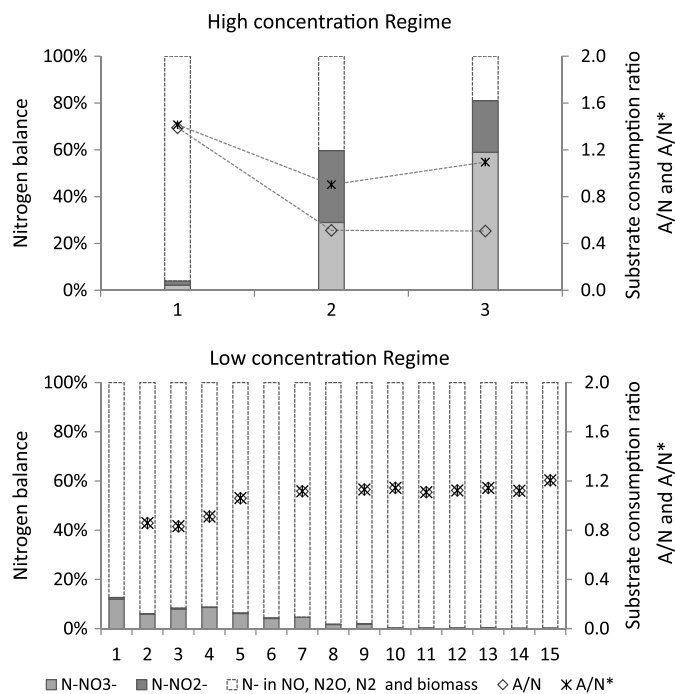


Fig. 6. Nitrogen balance, the consumption ratio between acetate and nitrate (A/N), and between acetate and total nitrate and nitrite (A/N*) throughout the experiments.

can be calculated from the nitrogen gas production. Once the gas content in the samples reaches its threshold and the gas production could not be monitored anymore, it is assumed that the nitrate consumption continues at a rate that is linearly extrapolated until the remaining nitrate concentrations reach zero. The results of calculated nitrate consumption and cumulative DIC production are presented in Fig. 7. This extrapolation assumes that substrate conversions in the low concentration regime were all completed before newly substrates were supplied.

The average NO₃⁻ consumption rates in a 1-h time interval and its standard deviation were calculated for each treatment period (the extrapolated values are not included). These results are presented in Fig. 8. The upper boundary of fastest NO₃⁻ possible rates

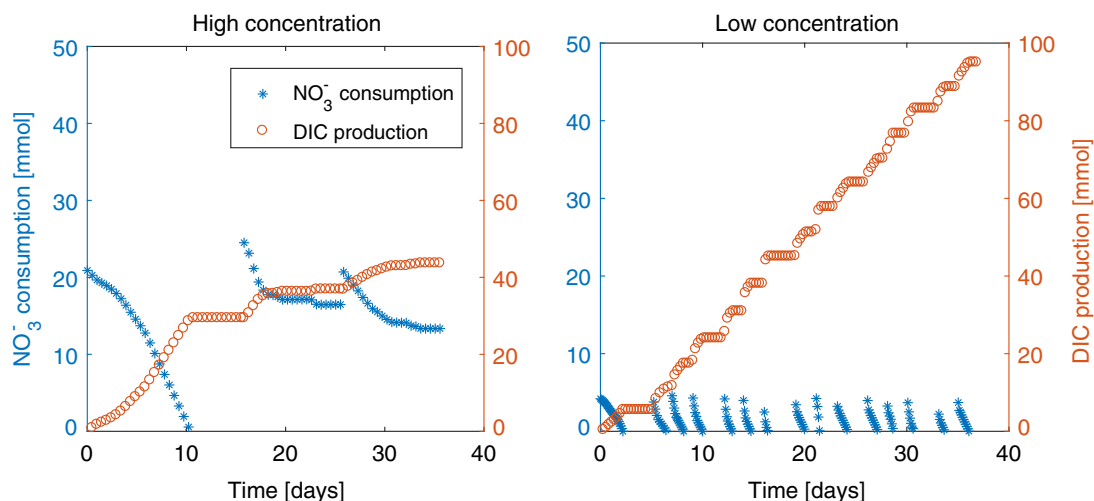


Fig. 7. Calculated NO₃⁻ consumption and DIC production from measured stoichiometric coefficients.

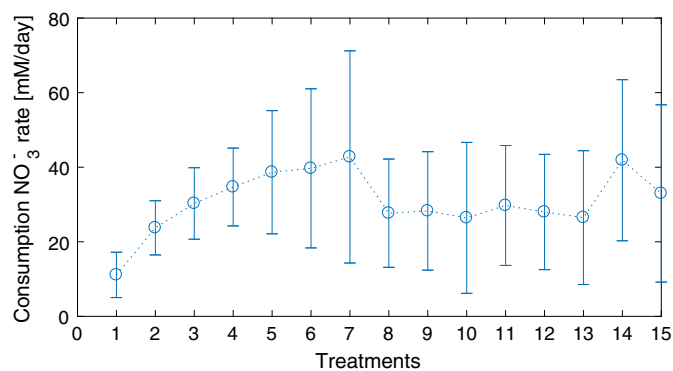


Fig. 8. Substrate consumption durations of the treatments in the low concentration regime.

corresponds with the measured rates in the beginning of the resident period, and the lower boundary of NO₃⁻ consumption rate corresponds with the measured rate when the gas production approached the gas content threshold. This analysis shows that NO₃⁻ consumption rates gradually increased during the first seven treatments, reaching a maximum average value of 42.7 mol/m³/day, corresponding to a CaCO₃ precipitation rate of 0.17% by weight/day. In the subsequent flushes, the consumption rate was reduced but still on average above 30 mol/m³/day. The highest gas production rate, which was recorded in the seventh treatment, corresponded to a nitrate conversion rate of 65 mol/m³/day or a precipitation rate of 0.26% by weight/day.

Amount of Precipitated CaCO₃

The total amount of precipitated calcium carbonate was calculated, resulting in 30.0 mmol for the high concentration regime and 71.5 mmol for the low concentration regime using the calcium measurements before and after each flush. In this calculation we assume mass conservation for calcium. The posttreatment analysis using 10% hydrogen chloride solution, presented in Fig. 9, showed that the average CaCO₃ content for the high concentration regime was about 0.28% by weight, which is 19.4 mmol CaCO₃. The distribution along the column did not show a clear trend. For the low concentration regime, the measured CaCO₃ content showed an uneven

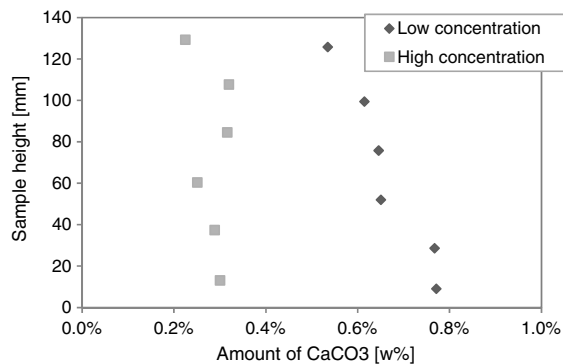


Fig. 9. Amount of CaCO_3 percentage by weight along the sand samples.

distribution along the column, ranging from 0.77% by weight close to the inlet at the bottom to 0.53% by weight close to the outlet at the top of the column. The average value was about 0.65% by weight, which is 44.1 mmol CaCO_3 . The difference between calculated and measured CaCO_3 content may be due to some precipitation in other parts of the setup (tubing, pressure controllers). Considering the target of 1% by weight precipitated CaCO_3 in the sand, the low concentration regime has better results than the high concentration regime.

Soil Behavior under Drained Monotonic Loading

Results of the drained triaxial compression tests are shown in Fig. 10. The treatment did not significantly increase the peak shear strength, but a clear increase was observed in small strain stiffness. The initial tangent modulus E of the treated sand in both regimes was more than doubled compared with the untreated control column. The effect of the gas phase was observed in the volumetric strain profile, (ϵ_{vol}), as the gas phase dampened the volumetric strain measured by the pore liquid changes of the samples. In the low concentration regime, the pore pressure profile dropped by several kilopascals. No significant pore pressure changes were observed for the control sample and for the high concentration regime. The initial pressure during shearing was about 2–3 kPa higher than the backpressure due to a difference in hydrostatic head.

ESEM Analysis of Dried Sand Lumps

ESEM analysis on a dried lump of sand from the third slice of the low concentration regime (Fig. 11) showed that a relatively low amount of large calcium carbonate crystals (up to 150 μm in diameter) was formed between the sand particles. Calcium carbonate crystals could be distinguished from sand particles by (1) the lighter gray value, indicating a slightly higher particle density, (2) their position between the other grains, being grown around the existing

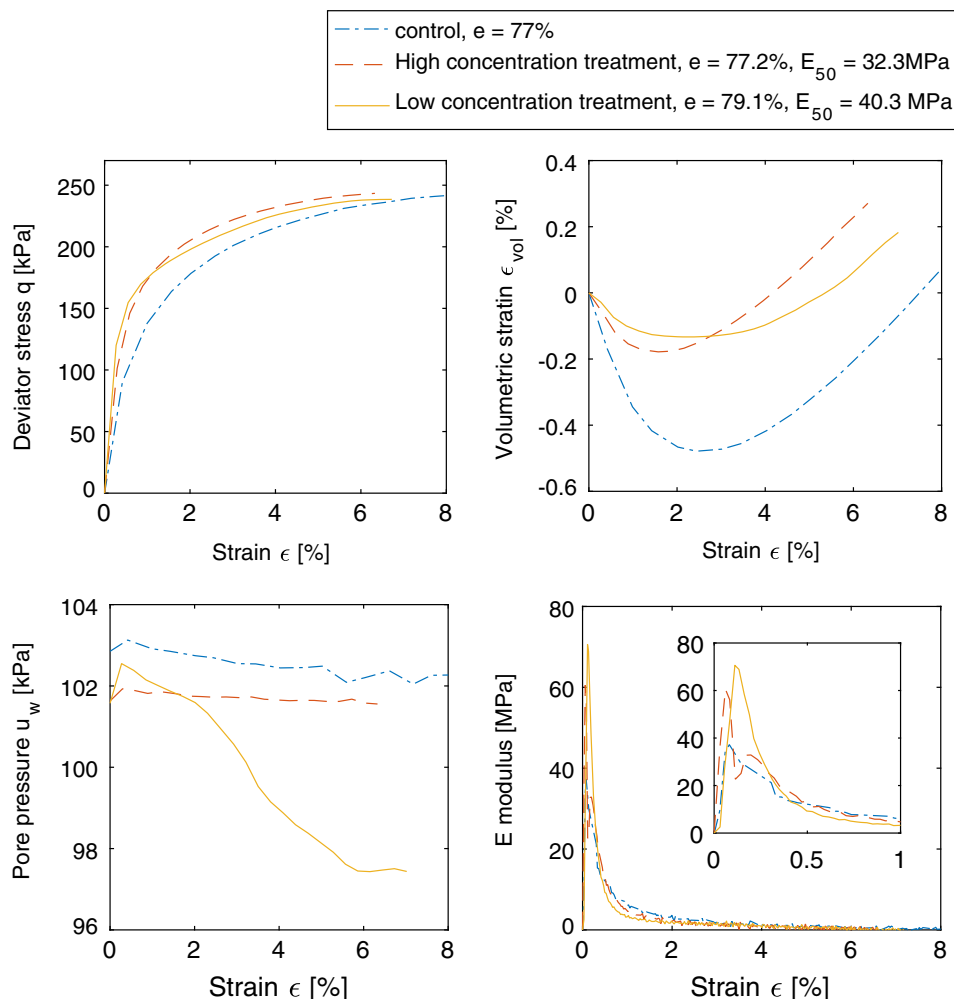
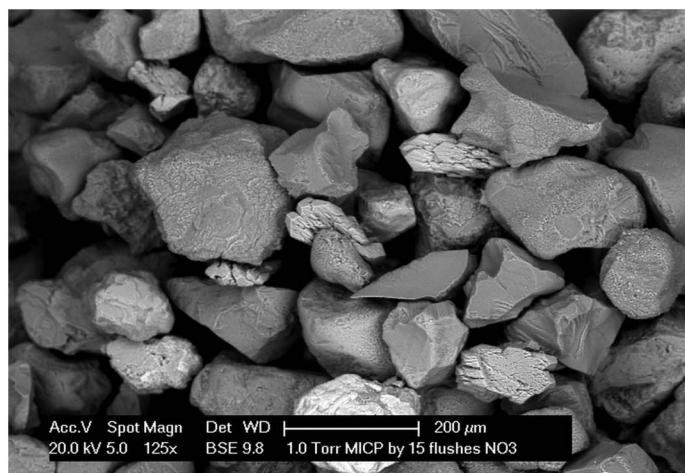
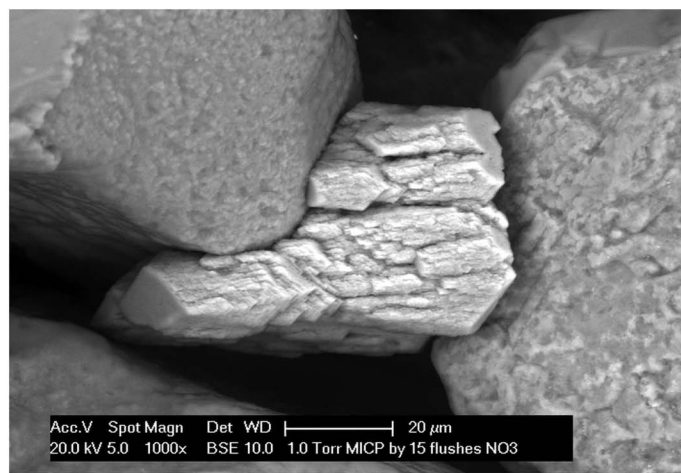


Fig. 10. Results from confined drained monotonic loading.



(a)



(b)

Fig. 11. ESEM image of a lump from the low substrate concentration regime. CaCO_3 precipitation (light gray) occurred heterogeneously, resulting in (a) few large crystals; and (b) their crystal structure appear to be hexagonal and grown in multiple phases.

sand grains, and (3) their rougher surface texture, probably indicating these crystals are calcite, which is grown in multiple phases. Energy-dispersive X-ray analysis on the crystals confirmed their main components to be calcium, carbon, and oxygen. X-ray diffraction analysis should be performed to confirm the crystals are indeed calcite.

Discussion

Effect of Initial Concentrations on the Conversion Rate and Yield

The experiments clearly show an effect of substrate concentration on the substrate consumption ratio and the overall conversion rate and efficiency. Although the two tested regimes started with the same inoculum of bacteria and the same ratio of the supplied substrates ($A/N = 1.2$, which corresponds to metabolic stoichiometry at maximum growth), the substrate consumption in the different concentration regimes was completely different.

Microbial growth was successfully stimulated in the low substrate concentration regime, which resulted in a high conversion rate and efficiency. With average conversion rates gradually increasing up to $40 \text{ mol/m}^3/\text{day}$ at the seventh flush and remaining between 20 and $40 \text{ mol/m}^3/\text{day}$ in the subsequent flushes, the nitrate consumption rate became significantly higher than the 7.5 mmol/L nitrate per day observed in the liquid batch incubation in Fig. 2. The consumed substrate ratio (A/N) was another indicator for microbial growth, as within four treatments it shifted from 0.8 for the liquid batch incubation toward 1.2. Another possible indication of active microbial growth was the significant reduction in hydraulic conductivity. Both regimes showed similar values of gas saturation ranging from 20 to 25% after the reaction phase to 10 to 15% after a flushing phase, which showed that part of the reduction in hydraulic conductivity was reversible. The gradually increasing irreversible reduction in hydraulic conductivity during the low concentration regime, which eventually resulted in clogging, may indicate that there must have been another material to fill the pores in addition to the induced gas phase. Microbial growth has been widely reported to significantly influence hydrodynamics of porous media, and can reduce sand permeability by up to three orders of magnitude (Baveye et al. 1998; Thullner et al. 2002; Gerlach and

Cunningham 2010). Considering the permeability reduction of the sand in the low concentration regime, biomass growth and accumulation can contribute to the irreversible part of the reduced hydraulic conductivity.

The high levels of nitrite, low A/N ratio, limited conversion rates, and efficiency observed in the high concentration regime are indications of strong inhibition or toxicity, and consequently, lack of biomass growth. We hypothesize that in this case, the gas phase could be unstable because there was no grown biomass to support its stability, which resulted in an almost completely reversible reduction in hydraulic conductivity. The difference in the end results of the two regimes confirms that a high substrate concentration is strongly related to loss of microbial activity, nitrite accumulation, and inhibition. This relation has been observed in other studies (Almeida et al. 1995; Sijbesma et al. 1996; Glass and Silverstein 1998; Dhamole et al. 2007). The nitrite reduction rate can initially be slower than the rate of nitrate reduction (Almeida et al. 1995). Therefore, when the microbial activity is not sufficient, a high dose of nitrate may cause nitrite to accumulate to an amount that in turn inhibits both cell growth and activity. Wang et al. (1995) showed with their experiments that after an initial proportional correlation up to $0.6 \text{ mmol/L NO}_3^-$, the net specific growth rate of a pure denitrifying culture decreases with increasing nitrate concentration. In the high concentration experiment of this current study, the negative effect of high substrate concentration was not evident in the first batch reaction period. However, for the subsequent second and third batch the bacteria in the high concentration regime had higher stress than those in the low concentration regime. Another reason for the observed inhibition in the second flush and third flush could be the long waiting time between the first and second batch. Complete consumption in the first batch caused a longer lag phase with low microbial activity, which according to Pirt (1975) can also be the cause of nitrite accumulation and loss of microbial activity when suddenly exposed to a high nitrate concentration.

The length of the lag phase and its consequences can be minimized by matching the hydraulic residence time to the substrate concentration and microbial activity. Another way to avoid a lag phase is by continuous supply of fresh substrates, as illustrated by the experiments of van Paassen et al. (2010a). They continuously flushed a 2-m sand column with a recycled solution initially containing 100 mmol/L calcium acetate and 120 mmol/L calcium

nitrate and found that all substrates were consumed within 10 days, which corresponds to a nitrate consumption rate of 24 mol/m³/day, without any detectable accumulation of nitrite. Moreover, using an enriched inoculum with a high concentration of bacteria is also useful in increasing its ability to deal with the stress of the lag phase (Pirt 1975) and therefore to limit nitrite accumulation. Erşan et al. (2015) also found that in the case of complete nitrate consumption, the measured nitrite concentration was inversely proportional to the cell concentration, and less leftover nitrite corresponds to a larger amount of CaCO₃ precipitation.

Effect of Other Process Conditions on Conversion Rate and Yield

The presence of calcium has an important effect on the metabolism of denitrifying organisms. Calcium carbonate precipitation is not only the chemical consequence of an alkalinity-producing bacterial metabolism in the presence of sufficient dissolved calcium, but it also provides a positive feedback on the metabolism. In the absence of precipitation, denitrification can cause the pH to increase to the upper limit of microbial denitrification, at which permanent nitrite accumulation occurs. Carbonate precipitation buffers the pH slightly below neutral and limits nitrite accumulation (Pham et al. 2018). Carbonate precipitation in the micro-environment of the bacterial cell could facilitate the cellular proton fluxes through the cell membrane and chemically favor the bacterial metabolism (Hammes and Verstraete 2002), similarly to root calcification of plants (McConnaughey and Whelan 1997). The interaction between carbonate precipitation and a robust microbial metabolism is also apparent in this current study. Although there was no analysis to verify the environmental conditions at microscale, results of complete substrate uptake, higher CaCO₃ precipitation yield, and indications of high cell concentration in the low concentration regime suggest that precipitation in itself can boost the overall performance through the positive feedback mechanism.

When comparing the liquid batch incubations with the sand column experiments, it shows that when the metabolism takes place in the sand, higher conversion rates and different substrate consumption ratios can be obtained. The positive effect on the performance of the denitrifying organisms is particularly evident for the low concentration regime, in which average nitrate consumption rates above 30 with a maximum value up to 65 mol/m³/day (as compared with 7.5 mol/m³/day for the liquid batch incubation) and substrate consumption ratios corresponding to conditions of maximum growth were observed. Whether this is due to the applied substrate ratio or concentration, difference in anaerobic conditions, or availability of granular surface that may create favorable micro-environments for the denitrifying organisms to grow or allow formation of biofilms as suggested by van Paassen et al. (2010a), cannot be concluded from these experiments.

The production of nitrogen gas also has an effect on the conversion. When pores are filled with nitrogen gas, liquid is expelled and the amount of available substrates is reduced. This may not affect the conversion rate, but it will influence the yield per volume of treated sand as observed by Pham et al. (2018), in which the parts of the columns that showed a higher gas saturation contained a lower calcium carbonate content. As the amount of produced gas is proportional to the consumed substrate, supplying high substrate concentrations in batch mode could cause the gas production to exceed its percolation threshold and lead to completely gas-filled zones or channels, disturbing homogeneous substrate supply.

Finally, the presence of other oxidizing agents, such as oxygen, ferric iron or sulfate, may also affect the denitrifying metabolism. For example, when substrates are supplied to the sand by surface

percolation, the air or oxygen present in the unsaturated zone may inhibit the denitrifying microbial activity or allow aerobic microorganisms to compete with denitrifying organisms for the available carbon source. The inhibiting effect of oxygen on the denitrification metabolism is well known (Ferguson 1994) and may be an alternative explanation for the loss in microbial activity during the second and third flush of the high concentration regime. During the first flush, the A/N ratio of the supplied substrates was 1.5, which is higher than the theoretical maximum A/N ratio corresponding to the stoichiometry for the denitrification metabolism at maximum growth. Still, all acetate appeared to be consumed when analyzing the expelled and flushed out liquid. In addition to potential measuring inaccuracies, the high acetate consumption may either indicate diffusion of substrates across the membrane or indicate the presence of an alternative electron acceptor, which could be dissolved oxygen in the cell water or pressure controllers. Verifying these suggested explanations requires additional research, in which potential adjustments to the triaxial setup need to be considered, such as the type of water used in the cell and the controllers or the diffusivity of the membrane.

Gas Production and Its Stability in the Sand

From the water saturation profiles of the treated sand columns, the produced gas created a gas saturation of about 20–30%, regardless of the consumed substrate amount. This is observed most clearly in the first treatment of the two regimes, in which all nitrate was consumed and only a little amount of nitrite had accumulated. As the consumed nitrate at the high concentration regime was five times higher than that at the low concentration regime, the amount of nitrogen gas produced was also expected to be five times higher. However, the difference in expelled liquid volume resulted in a gas saturation of 29 and 25% for the high and low concentration regimes, respectively, which was insignificant compared with the expected gas volume. The sand appeared to have a limited gas storage capacity, and when the produced gas exceeded this threshold, it vented from the sample to the back pressure controller. Similarly, transportation of excess nitrogen gas was also experimentally captured by Istok et al. (2007), who also could only obtain 23% gas saturation, which was significantly less than predicted based on their supplied amount of substrates. This discrepancy confirms that—under the conditions tested—the volume of produced gas was higher than the measured amount of gas in the sample, and excess gas had vented from the system. To leave the sample, the gas first needs to reach its percolation threshold and force an exit. Individual bubbles or isolated zones of gas either need to connect and form continuous gas-filled channels or the pressure in these isolated gas zones needs to exceed the air entry pressure of the narrow pore throats they need to squeeze through, to migrate upward. A similar process is required to allow the gas to flow through the tubing toward the back pressure controller.

The cyclic process of a decrease in water saturation by gas production followed by an increase in saturation by flushing shows a similar behavior, as seen during drying and wetting cycles in soils. As described by Fredlund et al. (2012), this process results in hysteresis of both the water content and hydraulic conductivity, which is attributed to the entrapped air that stays after the first drying–wetting cycle. For the tested soil of this study, the permanently entrapped air was about 10–15% of the pore volume in both the substrate regimes. Nevertheless, the flow rate patterns of the two regimes (Figs. 4 and 5) were significantly different, inferring a difference in the stability of this entrapped gas. The steady flow rates for the low concentration regime indicate that after flushing the distribution of the residual gas was not significantly influenced.

The entrapped air of this regime is therefore considered to be significantly more persistent under the tested hydraulic flow, possibly because of a more homogeneous distribution throughout the pore space. In contrast, the irregular flow rates observed during flushing in the high concentration regime appear to indicate that the gas is less stable and is redistributed during flushing. Apparently, the connectivity and persistence of the trapped gas is affected by the amount of gas produced during the first treatment. Other factors that may affect the distribution and persistence of the gas phase may include the soil properties, such as grain size distribution and sedimentary structure, and the rate and location at which the gas phase is introduced and trapped will affect the distribution of occluded gas (Baveye et al. 1998; Leroueil et al. 2015). The persistence of the trapped gas in the low concentration regime was also reflected by the pore pressure response during undrained loading and can be partly attributed to the formation of biofilms and microbial aggregations (Guelon et al. 2011). Although the presence of biomass in the pore space increases the resistance for both hydraulic and gas transport, the gas that is entrapped by the biomass is more stable and will lower the hydraulic conductivity even further.

Impact of the Reaction Products on the Sand Properties

The amount of precipitated CaCO_3 obtained during both regimes was not sufficient to significantly increase the peak strength under monotonic drained compressive loading. Nevertheless, the small amount of precipitated CaCO_3 did help to increase the soil stiffness and dilatancy, particularly at small strain, corresponding to a significant increase in tangent Young's modulus, which agrees with other results of MICP treatment on sandy soils (Feng and Montoya 2016; Lin et al. 2016). The limited response may be related to the size and distribution of the calcite crystals. As shown in the ESEM analysis, the low concentration regime resulted in large but isolated crystals, fitting between some but not all particle contacts. It appears that such crystals do not provide significant cohesive strength to the sand, but do increase dilatancy, corresponding to observations by van Paassen et al. (2012) or O'Donnell (2016). Still, drying the lumps of the treated sand from the low concentration regime still showed significant cohesive strength, considering light finger pressure was required to break the lumps under unconfined conditions. Part of the cohesive strength of the dried sample may be attributed to the biomass, as dried biofilms could provide a cohesive bond between particles (Guelon et al. 2011).

The role of the induced gas phase is clearly observed to affect the volumetric strain of the samples from both treated samples (Fig. 10). However, considering that the treated soils were partly saturated, the pore liquid changes in the sample may not be representative of the volumetric strain, as part of the volumetric strain may be caused by compression or venting of the gas. Various authors including He and Chu (2014) and O'Donnell et al. (2017b) showed that the presence of gas may significantly alter the soil behavior under undrained loading conditions. The compressible gas phase will dampen pore pressure buildup and may increase the undrained shear strength. The reduction in pore pressure for the low concentration regime indicates that the sample started to dilate and showed a slightly undrained response. Increased dilation may be the result to the CaCO_3 minerals formed between the sand particles as observed by O'Donnell et al. (2017a), and the undrained response may be caused by the reduced permeability due to the formation of biogas or biomass or a combination of both.

Overall, all of the reaction products, which are solid CaCO_3 minerals, gas phase and biofilms, can clearly alter the geotechnical behavior of the sand. The challenge is to optimize the ratio between the different products toward the desired behavior and to scale up the results from sample scale.

Implications for Practical Application of Denitrification-Based MICP

The results presented show that it is possible to optimize substrate concentration and substrate to nitrate ratio, to stimulate microbial growth and improve the conversion rate and efficiency. However, favoring microbial growth can lead to clogging before the target amount of calcium carbonate has been reached. This would require extra effort to force the liquid into the clogged areas. Clogging can be prevented by limiting microbial growth by controlling the overall substrate supply, but at the cost of a lower conversion rate or efficiency. If a large amount of CaCO_3 precipitation is the target, then the design needs to take into account the risk of clogging through microbial growth. First, the aim should be to stimulate the microbial growth until cell concentration and activity are sufficient. Subsequently, the aim should be to limit a further growth of the microbial population by changing the substrate concentration and acetate to nitrate ratio so that the system moves from one favoring growth toward one based on maintenance of the existing population only. This can be done by either increasing the nitrate concentration or lowering the acetate concentration, or increasing both the substrate concentrations, ensuring that the A/N ratio is less than 1.2 to increase the precipitation yield. The end results of the high concentration regime also showed that inhibition and nitrite accumulation can occur when the substrate to nitrate ratio is applied at the stoichiometry of the catabolic reaction. Therefore, the optimized A/N ratio for CaCO_3 precipitation should be between the ratio of maximum growth and pure maintenance, which are 1.2 and 0.6, respectively. Results of the batch liquid incubation and sand column experiments at the A/N ratio of 0.8 by van Paassen et al. (2010a) and Pham et al. (2018) showed that at this ratio it is also possible to maintain a robust metabolism with complete substrate consumption and limited accumulation of nitrite.

The observed precipitation rates for the low concentration regime are high compared with other reported rates in literature (van Paassen et al. 2010a; Kavazanjian et al. 2015). The low concentration regime achieved the result of 0.65% by weight in 5 weeks of treatments. However, all substrates were completely consumed during each step, and based on the rate of expelled volume of liquid within the reaction period, faster precipitation rates up to 0.26% by weight per day were observed. These high rates would improve the applicability of the process for soil reinforcement purposes.

Differences between the end results of the two regimes showed that stimulating microbial activity and minimizing the lag phase in the beginning of experiments is important for process performance, and as a result precipitation rate could be improved. Supplying the substrates at low concentrations proved to be effective for this target, but it requires more frequent flushing and increases the clogging potential. Consequently, it requires more work for contractors in the field. A high precipitation yield can practically be achieved with a high dose of substrate supply only after a phase in which microbial growth is stimulated using a dose of substrate at low concentrations.

An additional benefit of the method is the induced gas phase and biofilm aggregation to alter the geotechnical properties of sand. This study and others (Montoya and Dejong 2015; Lin et al. 2016) show that approximately 1.0% by weight of precipitated CaCO_3 supported by stably induced gas phase and biofilm can

be sufficient for soil stabilization, particularly in situations that do not require high peak strength (e.g., road or slope construction). Using the induced partially saturated state for liquefaction mitigation was demonstrated to be feasible (He et al. 2013; He and Chu 2014; Kavazanjian et al. 2015), and this desaturation state proved to be stable under a 1.5-m hydraulic gradient when it has the support from precipitated CaCO₃ and biomass aggregation. Persistence of biomass (Kim and Fogler 2000; Castegnier et al. 2006) leading to clogging is a drawback of the method, which limits supply of substrates for precipitation, but it could be a potential approach to create waste containment or seepage barriers (James et al. 2000) or mitigate issues of piping and leakage in an aquifer (Mitchell and Santamarina 2005; Ivanov and Chu 2008; Dejong et al. 2013). The possibility to select one of the three reaction products (CaCO₃, N₂-gas, and biomass) by adjusting the substrate supply regime allows tailoring the method for specific geotechnical applications.

Conclusions

In this study, different strategies for applying denitrification to stimulate the precipitation of calcium carbonate to improve the mechanical properties of sand have been evaluated. Selecting the appropriate substrate concentrations, inoculum, and environmental conditions are important to obtain fast reactions, high yield, and efficient use of resources. Appropriate choices make it possible to avoid accumulation of inhibiting intermediate products and to achieve the optimum final mechanical properties. The tests showed that low substrate concentrations result in higher calcium carbonate content and a well-maintained microbial activity. At high substrate concentrations, intermediate nitrogen compounds can accumulate, causing inhibition and reducing microbial activity. Providing an inoculum of denitrifying bacteria (bio-augmentation) helps to kick-off microbial activity at the start of experiments, obtain a high initial conversion rate, and minimize risks of inhibition during the process.

The obtained maximum precipitation rates of 0.26% by weight/day in this study may already be sufficient for practical ground improvement applications of denitrification-based MICP. The results of drained monotonic loading showed a significant increase in small strain stiffness at the obtained calcium carbonate contents of 0.28 and 0.65%. In addition to the strengthening effect from the precipitation, a significant fraction of gas appeared to be stable throughout the experiments, which can mitigate liquefaction by damping pore pressure buildup during undrained loading. Excessive biomass growth can cause clogging and may limit the substrate supply, but it also has the potential to be used for applications such as enhancing the stability of the gas phase and providing cohesive strength under dried conditions. All of the reaction products interact in changing the soil properties and can support or counteract each other in applications.

Acknowledgments

This research was funded by the Dutch Ministry of Economic Affairs, through STW perspective program BioGeoCivil (11337), and was performed in close collaboration with Deltares.

References

Almeida, J. S., S. M. Julio, M. A. M. Reis, and M. J. T. Carrondo. 1995. "Nitrite inhibition of denitrification by *Pseudomonas fluorescens*."

- Biotechnol. Bioeng.* 46 (3): 194–201. <https://doi.org/10.1002/bit.260460303>.
- Bayeve, P., P. Vandevivere, B. L. Hoyle, P. C. DeLeo, and D. S. de Lozada. 1998. "Environmental impact and mechanisms of the biological clogging of saturated soils and aquifer materials." *Crit. Rev. Environ. Sci. Technol.* 28 (2): 123–191. <https://doi.org/10.1080/10643389891254197>.
- Betlach, M. R., and J. M. Tiedje. 1981. "Kinetic explanation for accumulation of nitrite, nitric oxide, and nitrous oxide during bacterial denitrification." *Appl. Environ. Microbiol.* 42 (6): 1074–1084.
- Burbank, M. B., T. J. Weaver, T. L. Green, B. C. Williams, and R. L. Crawford. 2011. "Precipitation of calcite by indigenous microorganisms to strengthen liquefiable soils." *Geomicrobiol. J.* 28 (4): 301–312. <https://doi.org/10.1080/01490451.2010.499929>.
- Castegnier, F., N. Ross, R. P. Chapuis, L. Deschênes, and R. Samson. 2006. "Long-term persistence of a nutrient-starved biofilm in a limestone fracture." *Water Res.* 40 (5): 925–934. <https://doi.org/10.1016/j.watres.2005.12.038>.
- CEN (European Committee for Standardization). 2004. *Geotechnical investigation and testing: Laboratory testing of soil. 9: Consolidated tri-axial compression tests on water saturated soil*. ISO/TS 17892-9:2004. Brussels, Belgium: CEN.
- Chu, J., V. Stabnikov, and V. Ivanov. 2012. "Microbially induced calcium carbonate precipitation on surface or in the bulk of soil." *Geomicrobiol. J.* 29 (6): 544–549. <https://doi.org/10.1080/01490451.2011.592929>.
- Dejong, J. T., et al. 2009. "Upscaling of bio-mediated soil improvement." In *Proc., 17th Int. Conf. on Soil Mechanics and Geotechnical Engineering*, edited by M. Hamza, M. Shahien, and Y. El-Mossallamy. Alexandria, Egypt: IOS Press.
- Dejong, J. T., et al. 2013. "Biogeochemical process and geotechnical applications: Progress, opportunities and challenges." *Geotechnique* 63 (4): 287–301. <https://doi.org/10.1680/geot.SIP13.P.017>.
- Dhamole, P. B., R. R. Nair, S. F. D'souza, and S. S. Lele. 2007. "Denitrification of high strength nitrate waste." *Bioresour. Technol.* 98 (2): 247–252. <https://doi.org/10.1016/j.biortech.2006.01.019>.
- Erşan, Y. Ç., N. D. Belie, and N. Boon. 2015. "Microbially induced CaCO₃ precipitation through denitrification: An optimization study in minimal nutrient environment." *Biochem. Eng. J.* 101: 108–118. <https://doi.org/10.1016/j.bej.2015.05.006>.
- Feng, K., and B. M. Montoya. 2016. "Influence of confinement and cementation level on the behavior of microbial-induced calcite precipitated sands under monotonic drained loading." *J. Geotech. Geoenviron. Eng.* 142 (1): 04015057. [https://doi.org/10.1061/\(ASCE\)GT.1943-5606.0001379](https://doi.org/10.1061/(ASCE)GT.1943-5606.0001379).
- Ferguson, S. J. 1994. "Denitrification and its control." *Antonie van Leeuwenhoek* 66 (1–3): 89–110. <https://doi.org/10.1007/BF00871634>.
- Fredlund, D. G., H. Rahardjo, and M. D. Fredlund. 2012. *Unsaturated soil mechanics in engineering practice*. New York, NY: Wiley.
- Gerlach, R., and A. B. Cunningham. 2010. "Influence of biofilms on porous media hydrodynamics." Chap. 5 in *Porous media: Application in biological systems and biotechnology*, edited by K. Vafai, 173–230. Boca Raton, FL: CRC Press.
- Glass, C., and J. Silverstein. 1998. "Denitrification kinetics of high nitrate concentration water: pH effect on inhibition and nitrite accumulation." *Water Res.* 32 (3): 831–839. [https://doi.org/10.1016/S0043-1354\(97\)00260-1](https://doi.org/10.1016/S0043-1354(97)00260-1).
- Guelon, T., J.-D. Mathias, and P. Stoodley. 2011. "Advances in biofilm mechanics." Vol. 5 of *Biofilm highlights*, edited by H.-C. Flemming, J. Wingender, and U. Szewzyk, 111–139. Berlin, Germany: Springer.
- Hammes, F., and W. Verstraete. 2002. "Key roles of pH and calcium metabolism in microbial carbonate precipitation." *Rev. Environ. Sci. Biotechnol.* 1 (1): 3–7. <https://doi.org/10.1023/A:1015135629155>.
- He, J., and J. Chu. 2014. "Undrained responses of microbially desaturated sand under monotonic loading." *J. Geotech. Geoenviron. Eng.* 140 (5): 04014003. [https://doi.org/10.1061/\(ASCE\)GT.1943-5606.0001082](https://doi.org/10.1061/(ASCE)GT.1943-5606.0001082).
- He, J., J. Chu, and V. Ivanov. 2013. "Mitigation of liquefaction of saturated sand using biogas." *Geotechnique* 63 (4): 267–275. <https://doi.org/10.1680/geot.SIP13.P.004>.
- Heijnen, J. J., and R. Kleerebezem. 2010. *Bioenergetics of microbial growth: Encyclopedia of industrial biotechnology*. New York, NY: Wiley.

- Istok, J. D., M. M. Park, A. D. Peacock, M. Oostrom, and T. W. Wietsma. 2007. "An experimental investigation of nitrogen gas produced during denitrification." *Ground Water* 45 (4): 461–467. <https://doi.org/10.1111/j.1745-6584.2007.00319.x>.
- Ivanov, V., and J. Chu. 2008. "Applications of microorganisms to geotechnical engineering for bioclogging and biocementation of soil in situ." *Rev. Environ. Sci. Biotechnol.* 7 (2): 139–153. <https://doi.org/10.1007/s11157-007-9126-3>.
- James, G. A., B. K. Warwood, R. Hiebert, and A. B. Cunningham. 2000. "Microbial barriers to the spread of pollution." *Bioremediation*, edited by J. J. Valdes, 1–13. Dordrecht, Netherlands: Springer.
- Kavazanjian, E., S. T. O'Donnell, and N. Hamdan. 2015. "Biogeotechnical mitigation of earthquake-induced soil liquefaction by denitrification: A two-stage process." In *Proc., 6th Int. Conf. on Earthquake Geotechnical Engineering*. Christchurch, New Zealand.
- Kim, D.-S., and H. S. Fogler. 2000. "Biomass evolution in porous media and its effects on permeability under starvation conditions." *Biotechnol. Bioeng.* 69 (1): 47–56. [https://doi.org/10.1002/\(SICI\)1097-0290\(20000705\)69:1<47::AID-BIT6>3.0.CO;2-N](https://doi.org/10.1002/(SICI)1097-0290(20000705)69:1<47::AID-BIT6>3.0.CO;2-N).
- Leroueil, S., D. W. Hight, and A. R. Cabral. 2015. "Practical implications of gas-water interactions in soils." In Vol. 5. of *Proc., Geotechnical synergy in Buenos Aires 2015*, edited by A. O. Sfriso, D. Manzanal, and R. J. Rocca, 209–259. Alexandria, Egypt: IOS Press.
- Lin, H., M. T. Suleiman, D. G. Brown, and E. Kavazanjian Jr. 2016. "Mechanical behavior of sands treated by microbially induced carbonate precipitation." *J. Geotech. Geoenviron. Eng.* 142 (2): 04015066. [https://doi.org/10.1061/\(ASCE\)GT.1943-5606.0001383](https://doi.org/10.1061/(ASCE)GT.1943-5606.0001383).
- Martin, D., K. Dodds, I. B. Butler, and B. T. Ngwenya. 2013. "Carbonate precipitation under pressure for bioengineering in the anaerobic subsurface via denitrification." *Environ. Sci. Technol.* 47 (15): 8692–8699. <https://doi.org/10.1021/es401270q>.
- Matějů, V., S. Čížinská, J. Krejčí, and T. Janoch. 1992. "Biological water denitrification: A review." *Enzyme Microb. Technol.* 14 (3): 170–183. [https://doi.org/10.1016/0141-0229\(92\)90062-S](https://doi.org/10.1016/0141-0229(92)90062-S).
- McConnaughey, T. A., and J. F. Whelan. 1997. "Calcification generates protons for nutrient and bicarbonate uptake." *Earth Sci. Rev.* 42 (1): 95–117. [https://doi.org/10.1016/S0012-8252\(96\)00036-0](https://doi.org/10.1016/S0012-8252(96)00036-0).
- Mitchell, J. K., and J. C. Santamarina. 2005. "Biological considerations in geotechnical engineering." *J. Geotech. Geoenviron. Eng.* 131 (10): 1222–1233. [https://doi.org/10.1061/\(ASCE\)1090-0241\(2005\)131:10\(1222\)](https://doi.org/10.1061/(ASCE)1090-0241(2005)131:10(1222)).
- Montoya, B. M., and J. T. Dejong. 2015. "Stress-strain behavior of sands cemented by microbially induced calcite precipitation." *J. Geotech. Geoenviron. Eng.* 141 (6): 04015019. [https://doi.org/10.1061/\(ASCE\)GT.1943-5606.0001302](https://doi.org/10.1061/(ASCE)GT.1943-5606.0001302).
- O'Donnell, S. T. 2016. "Mitigation of earthquake-induced soil liquefaction via microbial denitrification: A two-stage process." Ph.D. dissertation, Arizona State Univ.
- O'Donnell, S. T., E. Kavazanjian, and B. E. Rittmann. 2017a. "MIDP: Liquefaction mitigation via microbial denitrification as a two-stage process. II: MICP." *J. Geotech. Geoenviron. Eng.* 143 (12): 04017095. [https://doi.org/10.1061/\(ASCE\)GT.1943-5606.0001806](https://doi.org/10.1061/(ASCE)GT.1943-5606.0001806).
- O'Donnell, S. T., B. E. Rittmann, and E. Kavazanjian. 2017b. "MIDP: Liquefaction mitigation via microbial denitrification as a two-stage process. I: Desaturation." *J. Geotech. Geoenviron. Eng.* 143 (12): 04017094. [https://doi.org/10.1061/\(ASCE\)GT.1943-5606.0001818](https://doi.org/10.1061/(ASCE)GT.1943-5606.0001818).
- Overmann, J., U. Fischer, and N. Pfenning. 1992. "A new purple sulfur bacterium from saline littoral sediments *Thiorhodovibrio winogradskyi* gen.nov. and sp.nov." *Arch Microbiol.* 157 (4): 320–335.
- Pham, V. P., A. Nakano, W. R. L. Van der Star, T. J. Heimovaara, and L. A. Van Paassen. 2018. "Applying MICP by denitrification in soils: A process analysis." *Environ. Geotech.* 5 (2): 79–93. <https://doi.org/10.1680/jenge.15.00078>.
- Pinar, G., E. Duque, A. Haidour, J. Oliva, L. Sanchez-Barbero, V. Calvo, and J. L. Ramos. 1997. "Removal of high concentrations of nitrate from industrial wastewaters by bacteria." *Appl. Environ. Microbiol.* 63 (5): 2071–2073.
- Pirt, S. J. 1975. *Principles of microbe and cell cultivation*. Oxford, UK: Blackwell Scientific.
- Rebata-Landa, V., and J. C. Santamarina. 2011. "Mechanical effects of biogenic nitrogen gas bubbles in soils." *J. Geotech. Geoenviron. Eng.* 138 (2): 128–137. [https://doi.org/10.1061/\(ASCE\)GT.1943-5606.0000571](https://doi.org/10.1061/(ASCE)GT.1943-5606.0000571).
- Sijbesma, W. F. H., J. S. Almeida, M. A. M. Reis, and H. Santos. 1996. "Uncoupling effect of nitrite during denitrification by *Pseudomonas fluorescens*: An in vivo 31P-NMR study." *Biotechnol. Bioeng.* 52 (1): 176–182. [https://doi.org/10.1002/\(SICI\)1097-0290\(19961005\)52:1<176::AID-BIT18>3.0.CO;2-M](https://doi.org/10.1002/(SICI)1097-0290(19961005)52:1<176::AID-BIT18>3.0.CO;2-M).
- Skempton, A. W. 1954. "The pore-pressure coefficients A and B." *Géotechnique* 4 (4): 143–147. <https://doi.org/10.1680/geot.1954.4.4.143>.
- Thullner, M., J. Zeyer, and W. Kinzelbach. 2002. "Influence of microbial growth on hydraulic properties of pore networks." *Transp. Porous Media* 49 (1): 99–122. <https://doi.org/10.1023/A:1016030112089>.
- van der Star, W. R. L., E. Taher, M. P. Harkes, M. Blauw, M. C. M. van Loosdrecht, and L. A. van Paassen. 2009. "Use of waste stream and microbes for in situ transformation of sand into sandstone." In *Ground improvement technologies and case histories*, edited by C. F. Leung, J. Chu, and R. F. Shen. Singapore: Research Publishing Services.
- van Paassen, L. A., C. M. Daza, M. Staal, D. Y. Sorokin, W. van der Zon, and M. C. M. van Loosdrecht. 2010a. "Potential soil reinforcement by biological denitrification." *Ecol. Eng.* 36 (2): 168–175. <https://doi.org/10.1016/j.ecoleng.2009.03.026>.
- van Paassen, L. A., R. Ghose, T. J. M. van der Linden, W. R. L. van der Star, and M. C. M. van Loosdrecht. 2010b. "Quantifying biomediated ground improvement by ureolysis: Large-scale biogROUT experiment." *J. Geotech. Geoenviron. Eng.* 136 (12): 1721–1728. [https://doi.org/10.1061/\(ASCE\)GT.1943-5606.0000382](https://doi.org/10.1061/(ASCE)GT.1943-5606.0000382).
- van Paassen, L. A., W. J. van Hermert, W. R. L. van der Star, G. van Zwieten, and L. van Baalen. 2012. "Direct shear strength of biologically cemented gravel." In *Proc., GeoCongress 2012: State of the Art and Practice in Geotechnical Engineering*, 968–977. Reston, VA: ASCE.
- van Spanning, R. J. M., D. J. Richardson, and S. J. Ferguson. 2007. "Introduction to the biochemistry and molecular biology of denitrification." Chap. 1 in *Biology of the nitrogen cycle*, edited by H. Bothe, S. J. Ferguson, and W. E. Newton, 3–II. Amsterdam, Netherlands: Elsevier.
- Wang, J. H., B. C. Baltzis, and G. A. Lewandowski. 1995. "Fundamental denitrification kinetic studies with *Pseudomonas denitrificans*." *Biotechnol. Bioeng.* 47 (1): 26–41. <https://doi.org/10.1002/bit.260470105>.
- Whiffin, V. S., L. A. van Paassen, and M. P. Harkes. 2007. "Microbial carbonate precipitation as a soil improvement technique." *Geomicrobiol. J.* 24 (5): 417–423. <https://doi.org/10.1080/01490450701436505>.
- Zumft, W. G. 1997. "Cell biology and molecular basis of denitrification." *Microbiol. Mol. Biol. Rev.* 61 (4): 533–616.